Effect of Surface Coating on Water Migration Into Resin-Modified Glass Ionomer Cements: A Magnetic Resonance Micro-Imaging Study

P. Jevnikar,[1] I. Serša,[2] A. Sepe,[2] O. Jarh,[2] and N. Funduk[1*]

Magnetic resonance micro-imaging was applied to study water diffusion into resin-modified glass ionomer cement restoration and to evaluate the effect of surface coating over restoration. Two cavities were prepared on the labial surface of extracted teeth and restored with resin-modified glass ionomer cement; one was protected with surface coating and the other was not. Immediately after restoration, the teeth were immersed in water. Progress of water diffusion into restorations was monitored by T_1 weighted spin-echo MRI at one-day intervals after the start of immersion. To quantify the water diffusion, a model was developed and compared with imaging data. Best fit yielded an effective water diffusion coefficient $D = (2.3 \pm 0.4)\ 10^{-12}$ m^2/sec. Experimental results demonstrated that surface coating protects the dental cement against water intrusion from the surface of the restoration which faces the oral cavity. Such coating, however, does not prevent water penetration from the dentine side. Magn Reson Med 44: 686–691, 2000. © 2000 Wiley-Liss, Inc.

Key words: magnetic resonance micro-imaging; glass ionomer cement; resin-modified; coating; water

Glass ionomer cements (GICs) are widely used dental materials because they bond adhesively to enamel and dentine (1) and release fluoride ions over a prolonged period of time. The setting mechanism of GIC has been described as an acid-base reaction between glass particles and an aqueous solution of a polymeric acid. In the process, the glass particles decompose and release Ca and Al ions, which later cross-link polyanions to form a matrix (2). GICs are water-based materials, so water plays an important role in the setting reaction. Besides being the reaction medium, water is also incorporated into the cement structure during the setting. If intraoral fluid comes into contact with cement before it has hardened, the matrix-forming ions (Ca and Al) are washed out, which leads to improper matrix formation (3) with inferior mechanical properties (4). For this reason, conventional GICs are susceptible to moisture contamination during the setting reaction. To prevent this, the application of surface coating over the restoration has been recommended (5). It was also found that light-cured, low-viscosity resins prevent water penetration better than do solvent-based varnishes (6,7). These coatings protect the material against water intrusion in the early stages of setting, and eliminate surface irregularities (8) as well as improve aesthetics of the restorations. Resin-modified glass ionomer cements (RM GICs) were developed (9) to overcome the moisture sensitivity of conventional GICs and to shorten the setting time. In these materials the water is partially replaced by hydroxy ethyl methacrylate (HEMA). Two reactions occur in the setting process: free radical polymerization of HEMA (which can be light or chemically initiated) and acid base reaction. The structure of RM GIC consists of a matrix of metal poly acrylate salts and of a polymer matrix (10). It is generally believed that RM GICs are less affected by moisture than are conventional GICs (11). Some manufacturers even claim that surface protection of RM GIC is not necessary. Different techniques were used to study the effectiveness of surface protection in RM GIC, including colorimetry (12), confocal microscopy (13), and mechanical testing (14,15). Magnetic resonance micro-imaging of water content in GICs has been reported as well (16).

Though RM GICs are said to be more resistant to early contamination by water than is conventional GIC, it is not clear whether they need to be protected against water penetration with a surface coating at all. The purpose of the present study was to visualize the water penetration into cavities restored with RM GIC, with and without surface protection. This was studied as a function of time using MR micro-imaging. In addition, a diffusion model was developed and compared with imaging data.

MATERIALS AND METHODS

Preparation of Teeth

Eight sound, caries-free, first upper human incisors of similar size and shape were selected for this study. Teeth were cleaned using a rubber cup and a fine pumice water slurry. The root canals were treated and sealed applying standard endodontic procedures. Access cavities were restored with a low-viscosity composite resin. Two experimental box-shaped Class V "cavities" were prepared on the labial surface of each tooth with a diamond burr mounted in a high-speed handpiece and cooled with a water spray. Both cavities were surrounded by sound enamel. Their dimensions were $4 \times 4 \times 2.5$ mm. Resin-modified glass ionomer FUJI II LC (GC, Batch 040477, Tokyo, Japan) was used to restore the cavities. An encapsulated form of FUJI II LC was selected to keep the powder/liquid ratio constant. Cavities were pretreated with the recommended conditioner. The cement was mixed according to the manufacturer's instructions, using a mechanical mixer, and placed in two layers. Each layer was cured for 20 sec with visible-light. Before curing the second layer, a cervical matrix was placed over the restoration to create a smooth surface. Immediately after light-curing, the resto-

[1]Department of Prosthodontics, Dental Clinic, Ljubljana, Slovenia.

[2]Jožef Stefan Institute, Ljubljana, Slovenia.

Grant sponsor: Ministry of Science and Technology, Slovenia; Grant number: J3-0047-0381-98.

*Correspondence to: Prof. Nenad Funduk, D.M.D., Ph.D., Department of Prosthodontics, Dental Clinic Hrvatski trg 6, SI-1000 Ljubljana, Slovenia. E-mail: nenad.funduk@ijs.si

Received 20 July 1999; revised 12 June 2000; accepted 13 June 2000.

rations were finished with superfine diamond burrs to remove excess material and polished with flexible discs, all under water spray. After finishing, the restorations were lightly air dried and the surface of each tooth was protected with Fuji Coat LC (GC, Batch 070741, Tokyo, Japan). Surface coating was applied with a brush, gently air dried, and light cured for 10 sec. The teeth were then immersed in distilled water, and stored at 37°C.

Model of Water Migration

A concentration gradient is a necessary condition for migration of water into a solid material matrix. Because of the concentration gradient, water molecules move toward a lower concentration, thereby establishing a flow is that is proportional to the gradient of concentration. The equation which defines such migration of molecules is not solvable analytically. For this reason we assume that migration is a diffusive process governed by an effective diffusion constant. The process of diffusion is governed by the diffusion equation (17):

$$\frac{\partial C}{\partial t} = D\Delta C, \qquad [1]$$

where C denotes the water concentration and D is the effective diffusion constant. Equation [1] can be solved analytically if sample geometry and boundary conditions are known.

In our model, the restoration is a rectangular parallel epiped. Since the cement is homogeneous and isotropic, the diffusion constant D is not position and orientation dependent. Two cases were considered: 1) the restoration is permeable on all six sides, or 2) the restoration is impermeable on the external side and permeable on the remaining five internal sides. The second model represents the restoration protected by coating. It is assumed that all sides, internal and external, are exposed to the same constant concentration of water. This assumes that the dentine and the oral cavity provide equal supply of water to the restoration. This assumption appears to be adequate, since it is known from the literature (18) that the apparent diffusion coefficient of water in dentine is approximately 100 times larger than in resin-based glass-ionomer cements. The initial condition for both models is that there is no free water in the sample at $t = 0$. Upon inspection of Fig. 1, the assumption appears to be a good one, although the water intake from the oral cavity is slightly faster than from the dentine.

The water in dentine has a very short relaxation time (19) and cannot be detected with the spin-echo imaging sequence used in our experiments. For water diffusing into the restoration from all six faces, the solution of Eq. [1] is given by Crank (17):

$$C_{6F}(x,y,z,t;a,b,c) = C_0(1 - P_{++}(x,t;a)P_{++}(y,t;b)P_{++}(z,t;c)). \qquad [2]$$

Here C_0 denotes the final concentration of water in the restoration (dimensions $a \times b \times c$), and $P_{++}(x,t;a)$, $P_{++}(y,t;b)$, $P_{++}(z,t;c)$ are normalized 1D diffusion profiles

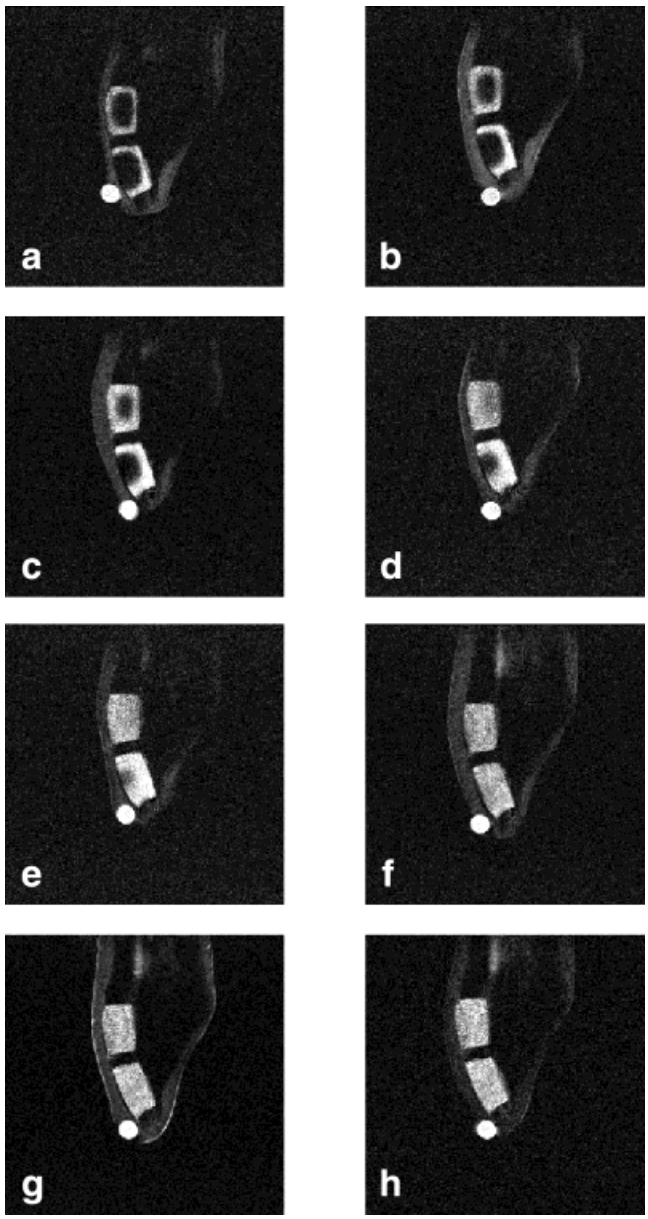

FIG. 1. MR micro-images of surface protected (lower restoration of each MR micro-image)and unprotected (upper restoration of each MR micro-image) RM GIC restorations recorded after: 24 (**a**), 36 (**b**), 48 (**c**), 72 (**d**), 96 (**e**), 120 (**f**), 144 (**g**), and 192 (**h**) hr of immersion in water. Images were acquired with spin-echo imaging technique. The imaging parameters were: FOV = 2 cm, slice thickness = 2.5 mm, TE = 18 msec, and TR = 400 msec. A standard sample was used to renormalize all images to its signal intensity.

at time t in directions x, y, and z, respectively. The normalized profile $P_{++}(x,t;a)$ corresponds to the solution of the diffusion equation (Eq. [1]) in 1D where water diffuses in the x direction, outwards from a sample having the surfaces perpendicular to x axis permeable and all other surfaces impermeable to diffusion. This problem is the reverse of water diffusion into the restoration, where water diffuses into the restoration volume. The normalized 1D solution to such a reverse diffusion problem is $1 - P_{++}(x,t;a)$. Initially, at $t = 0$, the water concentration is uniform

within the sample of thickness a, so that $P_{++}(x, t = 0; a) = 1$ for $0 < x < a$, whereas the water concentration on both surfaces is equal to 0 at any time t that is: $P_{++}(x = 0, t; a) = 0$ and $P_{++}(x = a, t; a) = 0$. The solution is

$$P_{++}(x,t;a) = \sum_{n=0}^{\infty} \frac{4}{\pi(2n+1)} \sin\left(\frac{(2n+1)\pi x}{a}\right) \times \exp\left(\frac{-(2n+1)^2\pi^2 Dt}{a^2}\right). \quad [3]$$

The 1D profiles $P_{++}(y,t;b)$ and $P_{++}(z,t;c)$ have the same form as Eq. [3].

An analogous solution to Eq. [2] is obtained also for water diffusion in the restoration of dimensions $a \times b \times c$ having the external face at $x = 0$ impermeable to diffusion and the five "internal" faces permeable to diffusion

$$C_{5F}(x,y,z,t;a,b,c) = C_0(1 - P_{\pm}(x,t;a)P_{++}(y,t;b)P_{++}(z,t;c)). \quad [4]$$

Equation [4] differs from Eq. [2] in normalized 1D diffusion profile $P_{\pm}(x,t;a)$. This is the solution for the 1D diffusion process in the x direction, where water diffuses a rectangular sample volume outwards through a side at $x = a$, which is the only side permeable to diffusion. Again, the water concentration in the sample at time $t = 0$ is uniform, so that $P_{\pm}(x, t = 0; a) = 1$ for $0 < x < a$ and is equal to 0 on the surface $x = a$ at all times t and $P_{\pm}(x = a, t; a) = 0$. Since the diffusion is proportional to the derivative of the normalized profile on the spatial coordinate, the following condition $\partial P_{\pm}(x,t;a)/\partial x = 0$ applies to the side at $x = 0$, which is impermeable. The solution for the normalized 1D diffusion profile satisfying the above initial and boundary conditions is

$$P_{\pm}(x,t;a) = \sum_{n=0}^{\infty} \frac{4}{\pi(2n+1)} \cos\left(\frac{(2n+1)\pi x}{2a}\right) \times \exp\left(\frac{-(2n+1)^2\pi^2 Dt}{4a^2}\right). \quad [5]$$

The solution for 1D diffusion given by Eqs. [3] and [5] is a weighted sum of many terms, with a sine spatial modulation and an exponential time decay, each being an eigenfunction of the diffusion equation (Eq. [1]). The weights in the sum are determined by the projection of the initial concentration profile upon the infinite set of eigenfunctions. In our model, the initial concentration profile is a step function equal to 1 within the sample. It is equal to 0 outside it, and the weights are inversely proportional to the frequency $(2n + 1)$ of the sine modulation. Besides, each eigenfunction in the sum decays with a different time constant, which is inversely proportional to D and proportional to the square of the modulation period $a/(2n + 1)$. Since terms with high spatial modulation decay much faster that those with low modulation, any initial concentration profile with sharp concentration changes becomes rounded off as time progresses. This is especially true in our case, in which the initial profile is a step function.

MR Micro-Imaging

Experiments were performed on a Bruker Biospec system with a 100 MHz horizontal bore magnet (Oxford Instruments Ltd., Oxford, UK) equipped with micro-imaging capabilities. T_1 weighted spin-echo imaging sequence with repetition time (TR) of 400 msec and echo time (TE) of 18 msec was used. A relatively long TE was used because of hardware limitations. Image data were acquired using a resolution reduction factor of 2 in the phase-encoding direction; thus, for the image with a 256 × 256 matrix only 128 phase-encoding steps were needed. To improve the signal-to-noise ratio, each image was an average of 36 acquisitions, which prolonged scanning time to 31 min per image. To prevent dehydration during the imaging procedure, each tooth was encapsulated prior to imaging in a micro-tube sealing wax. This was removed immediately after imaging, and the tooth was immersed in water until the next imaging procedure. The encapsulating medium had a negligible proton signal intensity compared to the signal intensity of water imbibed into the restorations. The 2.5-mm-thick slice, with a 20-mm field of view, was set at the center of the labial surface in the sagittal direction. An insert was constructed which enabled identical slice positioning in all experiments. A small tube containing a mixture of normal and deuterated water in a 1:4 ratio was added to the incisal margin in all measurements. This standard was used to normalize the MR signals from different experiments. The mixture of normal and deuterated water was necessary to reduce the strength of the water proton signal that would otherwise overwhelm the weaker signal from water in the glass ionomer cement. The first series of images was taken 24 hr after the start of cement mixing, the second one after 36 hr. The subsequent images were recorded at 48, 72, 96, 120, 144, and 192 hr.

Quantitative Analysis of Diffusion Profiles

Experimental MR micro-images were analyzed and compared to the images calculated with the above diffusion model. The model fit the observed patterns well. In addition, an effective diffusion coefficient was obtained. The 2D digital micro MRI provided good visualization of the spatial distribution of water in RM GIC and how it changes with time. To compare the model of the restoration in contact with water on all six surfaces (Eq. [2]) with experimental images, all micro-images of the teeth that were recorded at different times were normalized with respect to the signal of the H_2O/D_2O standard. Then the total signal from the RM GIC without protective coating was calculated by adding up pixel intensities across the whole restoration. Next, this was divided by the number of pixels in the cement region so that the average image signal intensity in a particular cement region was obtained. This average signal is exactly proportional to the amount of water in the selected region of dental cement.

After several days of immersion, the water concentration reached its final value C_0 everywhere in the restoration. A

relative average water concentration is the ratio of the average $\bar{C}_{6F}$ and the final water concentration C_0. In our experiment it was assumed that 192 hr after the immersion in water, the average water concentration in resin-modified glass ionomer cement equals the final water concentration C_0. Experimental errors σ of the relative average water concentrations were calculated as ratios between the image noise and the signal level of the final water concentration C_0.

The diffusion model gives the relative average water concentration ($\bar{C}_{6F}/C_0$) in RM GIC. This is an integral of water concentration C_{6F} (Eq. [2]) over the image, divided by the product between the area of the integration ($a\,b$) and the final water concentration C_0

$$\bar{C}_{6F}/C_0 = \frac{1}{abC_0}\int_0^a dx \int_0^b dy\; C_{6F}(x,y,c/2,t)$$

$$= 1 - \bar{P}_{++}(t;a)\bar{P}_{++}(t;b)P_{++}(c/2,t;c). \qquad [6]$$

In Eq. [6] the relative average water concentration is calculated for the imaging slice at position $z = c/2$, whereas $\bar{P}_{++}$ denotes the relative average water concentration of a 1D diffusion profile P_{++} (Eq. [3]), which can be written as

$$\bar{P}_{++}(t;a) = \frac{1}{a}\int_0^a dx\; P_{++}(x,t;a)$$

$$= \sum_{n=0}^{\infty} \frac{8}{\pi^2(2n+1)^2}\exp\left(\frac{-(2n+1)^2\pi^2 Dt}{a^2}\right). \qquad [7]$$

For known dimensions of the restorations, equations for the relative average water concentration are dependent only on time, and have the effective diffusion coefficient as a free parameter. The diffusion coefficient was determined from the best fit of the theoretical model (Eqs. [6] and [7]) to the experimental relative average water concentration.

RESULTS

Water diffusion into RM GIC restorations that was monitored by MR micro-imaging applied at different immersion times is shown in Fig. 1. After 24 hr of immersion in water, the lower restoration (protected with surface coating) and the upper restoration (unprotected) show different behaviors (Fig. 1a). In the unprotected sample, water diffused into the material from pulpal and axial dentinal walls and from the surface of the restoration facing the oral cavity. Signal intensities indicate similar diffusion from all directions. In the restoration with the protected surface, the water diffusion from pulpal and axial walls is comparable to the unprotected RM GIC; however, there is no signal corresponding to the water diffusing through the coated surface of the cement. The difference in water diffusion patterns between the two restorations is observable also after 36 hr (Fig. 1b) and 48 hr (Fig. 1c) of immersion. At 48 hr the signal bands are broader and less sharp, indicating smearing of the water front. After 72 hr (Fig. 1d) the water reaches the center of the unprotected restoration. At this time the signal intensity is equal in all directions. On the other hand, at 72 hr the diffusion into the protected restoration is not yet completed. Water penetration from the axial directions contributes to the MR signal at the incisal and gingival third of the surface. This effect is more pronounced after 96 hr (Fig. 1e). After 120 hr of immersion the MR signal is spread homogeneously throughout both restorations (Fig. 1f). There is a very small increase in signal intensity after 144 hr (Fig. 1g) and none at 192 hr (Fig. 1h), when the experiment was terminated.

Relative average water concentrations calculated from the recorded MR micro-images of the unprotected RM GIC (upper restorations in Fig. 1a–h) and the modeled values are presented in Fig. 2. The effective diffusion coefficient was determined by fitting the proposed model (Fig. 2, solid line) to the experimental data (Fig. 2, points) in the unprotected restoration, Eq. [6]. The relative average water concentrations were calculated using the first 100 terms in Eq. [7]. The error due to truncation of terms in Eq. [7] is the highest (0.2%) at the beginning of diffusion ($t = 0$), when all diffusion exponential factors are equal to 1. The error is considerably lower at later times due to the rapid decrease of exponential diffusion factors in higher terms. Best fit between the model and the experiment yields the diffusion coefficient $D = (2.3 \pm 0.4)\ 10^{-12}$ m^2/sec, which was used to simulate diffusion profiles (Fig. 3). For these simulations the following conditions from the experiment, shown in Fig. 1, were taken: the model sample size corresponds to the actual dimensions of restoration (a = 2,5 mm, b = 4 mm, and c = 4 mm), and the slice position and orientation to the imaging slice at $z = c/2$.

DISCUSSION

MR micro-imaging allows a direct visualization of water penetration in the material without using dyes that have a

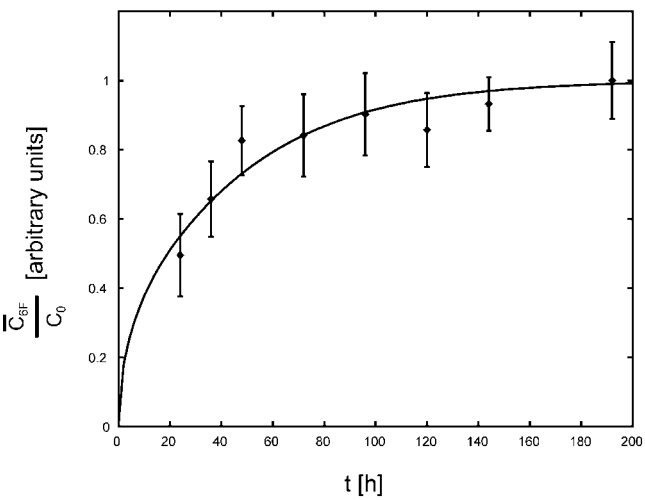

FIG. 2. Best fit between the experimentally obtained relative average water concentrations $(\bar{C}_{6F}/C_0)_{measured}$ (points) and theoretical model given by Eqs. [2] and [6] (continuous curve). Best fit between the model and the experimental data yielded a diffusion coefficient $D = (2.3 \pm 0.4)\ 10^{-12}$ m^2/sec.

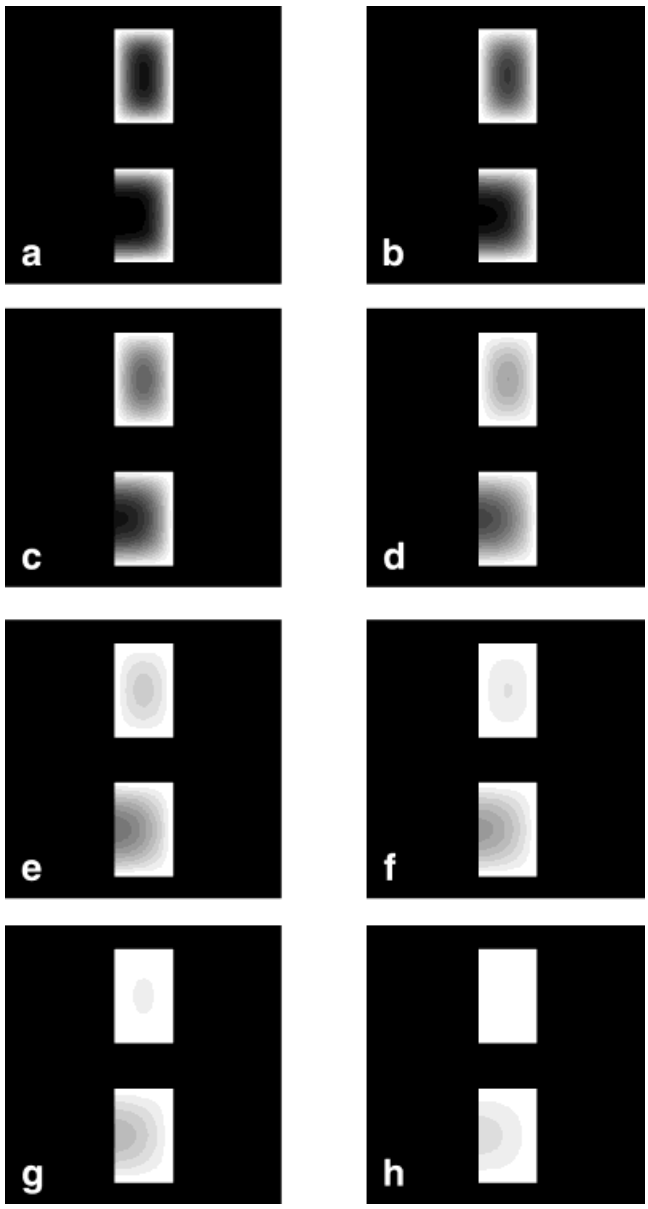

FIG. 3. Simulated diffusion profiles calculated from the diffusion models in surface protected restoration Eq. [4] (lower profile on each figure) and unprotected restoration Eq. [2] (upper profile in each figure). Profiles were calculated for the same geometry, slice position and times of immersion (24 (**a**), 36 (**b**), 48 (**c**), 72 (**d**), 96 (**e**), 120 (**f**), 144 (**g**), and 192 (**h**) hr), as in the experiment in Fig. 1; diffusion coefficient in simulation was $D = 2.3\ 10^{-12}$ m^2/sec.

higher molecular weight than water, so their diffusion is likely to be slower. In addition, the integrity of the specimens is also maintained and the appropriate slice positioning gives the information in a direction most suitable for the given geometry. There is no need for sectioning and dehydration of the specimens, as is the case with SEM and optical microscopy. Thus, the samples can be examined in an environment that resembles the clinical conditions reasonably well. In addition, the technique enables us to monitor the whole process on the same sample, and the same sample can be examined by another method if necessary.

Because of short T_2 the protons in dentine do not contribute to the MR signal detected with echo at 18 msec, and consequently dentine appears dark on MR micro-images. This is in agreement with Funduk et al. (19), who reported that the fluid in dentinal tubules does not contribute to the MR signal if the TE of the pulse sequence exceeds 3 msec, since the water proton spin-spin TR (T_2) in dentine is on the order of 500 μs. Sensitivity of the method can be further increased by shortening of the TE. Increased sensitivity would allow a shorter scan time and thus enable better coverage of concentration profile measurements.

Our preliminary studies showed that soft tissues and fluid in the pulp cavity produce a very strong MR signal that overwhelms the imaging of water in RM GIC. For this reason, root canals had to be endodontically treated and obturated. This limited our study, since in freshly extracted teeth with intact pulps, adequate perfusion with capillary flow might speed up the diffusion into the restorations.

Conventional GICs are very sensitive to early contact with water. In the RM GICs the photo-polymerization has been claimed to protect the material from moisture contamination during the initial stage of the setting process. Our results show that fast initial photo-polymerization setting does not prevent water uptake. This has been proven experimentally (Fig. 1) as well as by comparing a diffusion model with experimental data (Fig. 3). The model is based on certain assumptions that do not exactly match the experimental conditions, namely that the shape of the cavity is exactly rectangular. Good agreement with the experimental data, however, confirms that the assumptions are reasonable and that such a model could be used to describe the diffusion process in hard tissue in general.

If the extrinsic fluid comes in contact with the glass ionomer system during early setting, it may disrupt the water balance and impair the acid base setting reaction, eluting the reactants (3,20). The acid base reaction in RM GIC is slower than in conventional glass ionomers, since poly HEMA matrix formed immediately after photo-polymerization reduces the setting rate (21). Thus in this type of GIC early contact with excess water might also dissolve soluble ions and impair the acid-base part of the setting mechanism. In addition, HEMA is a hydrophilic molecule that enhances water sorption.

In this study, water diffusion in RM GIC was compared in two types of restorations: those protected with a surface coating and those left unprotected. By comparing the two restorations, the efficacy of the coating and the duration of its preventive effect was evaluated. It was demonstrated that the application of a surface coating protected the cement from water diffusion from the surface of the restoration for 48 hr or longer. However, the diffusion of water from pulpal surfaces of the restoration brought water into the restoration. After 72 hr of immersion in water, the MRI signal was present in the lower and upper part of the surface of the coated cavity (Fig. 1d). This signal was interpreted as originating from water diffusing from the dentine.

The reported experiments show that water diffuses into RM GIC restorations from both the oral cavity and dentine. It is documented that early contact with water is harmful for the surface of the GIC exposed to the oral cavity be-

cause the acid-base reaction is impaired. As a consequence, disintegration of the surface structure, discoloration, and increased surface roughness occur (22). Acid-base reaction is a slow process, most of which is completed in a few hours (23). Based on the results of our study, the application of surface coating over the RM GIC restorations is strongly recommended, since it protects the restoration during early setting of the cement. However, the coating prevents water migration into the GIC from the surface only. After a time, the water migration from the dentinal sides of the restoration reaches the outer surface. However, by that time the outer surface is well hardened. It is undetermined whether water entering from the dentine affects the acid-base setting of the restoration. It should be kept in mind that at restoration dentine interfaces the water is present in pores, which limits the leaching of ions from the restoration.

ACKNOWLEDGMENTS

The authors thank Prof. Mik M. Pintar for his critical reading of the manuscript.

REFERENCES

1. Mitra SB. Adhesion to dentin and physical properties of a light-cured glass ionomer base. J Dent Res 1991;70:72–74.
2. Crisp S, Pringuer MA, Wardleworth D, Wilson AD. Reactions in glass ionomer cements: an infrared spectroscopic study. J Dent Res 1974;53: 1414–1419.
3. Anstice HM, Nicholson JW. Studies on the structure of light cured glass ionomer cements. J Mater Sci Mater Med 1992;3:447–451.
4. Mojon P, Kaltio R, Feduik D, Hawbolt EB, MacEntee ML. Short-term contamination of luting cements by water and saliva. Dent Mater 1996; 12:83–87.
5. Causton BE. The physico-mechanical consequences of exposing glass ionomer cements to water during setting. Biomaterials 1981;2:112–114.
6. Earl MSA, Hume WR, Mount GJ. Effect of varnishes and other surface treatments on water movement across the glass-ionomer cement surface. Aust Dent J 1985;30:298–301.
7. Earl MSA, Mount GJ, Hume WR. The effect of varnishes and other surface treatments on water movement across the glass-ionomer cement surface II. Aust Dent J 1989;34:326–329.
8. Hotta M, Hirukawa H, Aono M. The effect of glaze on restorative glass-ionomer cements: evaluation of environmental durability in lactic acid solution. J Oral Rehabil 1995;22:685–689.
9. Mitra SB. Photo curable ionomer cement systems. European Patent Application No. 88312127.9, publication No. 0323120; 1989.
10. Wilson AD. Resin-modified glass-ionomer cements. Int J Prosthodont 1990;3:425–429.
11. Cho E, Kopel H, White SN. Moisture susceptibility of resin-modified glass-ionomer materials. Quint Int 1995;26:351–358.
12. Hotta M, Hirukawa H, Yamamoto K. Effect of coating materials on restorative glass-ionomer cement surface. Oper Dent 1992;17:57–61.
13. Watson T, Banerjee A. Effectiveness of glass-ionomer surface protection treatments: a scanning optical microscope study. Eur J Prosthodont Rest Dent 1993;2:85–90.
14. Miyazaki M, Moore BK, Onose H. Effect of surface coatings on flexural properties of glass ionomers. Eur J Oral Sci 1996:104:600–604.
15. Williams JA, Billington RW, Pearson GJ. Effect of moisture protective coatings on the strength of a modern metal-reinforced glass-ionomer cement. J Oral Rehabil 1998;25:535–540.
16. Jevnikar P, Jarh O, Sepe A, Pintar MM, Funduk N. Micro magnetic resonance imaging of water uptake by glass ionomer cements. Dent Mater 1997;13:20–23.
17. Crank J. The mathematics of diffusion, 2nd ed. Oxford: Clarendon Press; 1975. p 11–27.
18. Petelin M, Skalerič U, Cevc P, Schara M. The permeability of human cementum in vitro measured by electron paramagnetic resonance. Arch Oral Biol 1999;44:259–267.
19. Funduk N, Kydon DW, Schreiner LJ, Peemoeller H, Miljkovič L, Pintar MM. Composition and relaxation of the proton magnetization of human enamel and its contribution to the NMR image. Magn Reson Med 1984;2:66–75.
20. Shen C, Grimaudo N. Effect of hydration on biaxial flexural strength of a glass ionomer cement. Dent Mater 1994;10:190–195.
21. De Gee AJ, Leloup G, Werner A, Vreven J, Davidson CL. Structural integrity of resin-modified glass ionomers as affected by the delay of omission of light activation. J Dent Res 1998;77:1658–1663.
22. Hotta M, Hirukawa H, Aono M. The effect of glaze on restorative glass-ionomer cements: evaluation of environmental durability in lactic acid solution. J Oral Rehabil 1995;22:685–689.
23. Wilson AD, Nicholson JW. Acid-base cements. Cambridge: Cambridge University Press; 1993. p 134–143.